Journal of Molecular Catalysis A: Chemical 288 (2008) 52–57

Contents lists available at ScienceDirect

Journal of Molecular Catalysis A: Chemical

journal homepage: www.elsevier.com/locate/molcata

Exchanged zeolites with transition metals of the first period as photocatalyts for *n*-hexadecane degradation

Ahmed K. Aboul-Gheit*, Sahar M. Ahmed, Samia A. Hanafy

Egyptian Petroleum Research Institute, P.O. Box 9540, Cairo 11787, Nasr City, Egypt

ARTICLE INFO

Article history:
Received 3 January 2008
Received in revised form 5 March 2008
Accepted 5 March 2008
Available online 21 March 2008

Keywords:
Transition metals
Zeolites
Photodegradation
n-Hexadecane

ABSTRACT

The photodegradation of *n*-hexadecane (*n*-C_{16}) was tested using photocatalysts containing MOR, ZSM-5 or Y zeolites exchanged with ~5.2 wt% of V, Cr, Mn, Cu or Zn. *n*-C_{16} was selected to realize intimate contact to the metal cations inside the zeolitic channels. X-ray diffraction (XRD) and Fourier transform infrared (FTIR) indicated retaining high crystallinity of the catalysts incorporating the current metals. Moreover, the UV–vis spectra indicated that the current-exchanged metals are present as isolated species. Application of the Langmuir–Hinshelwood kinetics admitted calculating the photocatalytic degradation rate constant, *k*, and the adsorption coefficient, K_{ad}, for the photodegradation of *n*-hexadecane, which have been found to correlate with atomic weights of the metals and their active cationic surface area. The MOR containing catalysts exhibited a reversed behaviour of *k* and K_{ad}, compared to those containing ZSM-5 and Y zeolites. However, K_{ad} seems to be correlated well with the active surface area of the metal cations.

1. Introduction

Zeolites are microporous microcrystalline inorganic materials capable of adsorbing organic molecules [1,2]. They possess regular periodic structures with channels and cages extending regularly allover their structure. Adsorption of organic guest molecules may occur both on the external and internal surfaces of a zeolite crystal. Intracrystalline adsorption occurs by diffusion of the guest molecule into the channels and cavities of the zeolite only when the kinetic diameter of the guest molecule is smaller than the diameter of the cavity. Normally, molecular alignment and conformational restrictions occur on guest molecules, which are particularly significantly effective in zeolites photoactivity.

Cations (e.g., Na) located in the zeolite cages, channels and cavities, can be exchanged by other cations. The size, number and position of the exchanged cations contribute significantly to the catalyst activity. The cation locations depend on the guest molecule, e.g., shape and free volume of the supercage within X and Y zeolites [3] could decide the nature of a product obtained from a guest molecule. The volume available for a guest molecule in a supercage depends on the number and nature of the cations, i.e., decreases as the cation size increases from Li to Cs [4]. The interaction between a guest molecule and the cavity differs from weak Van der Waals forces to hydrogen bond to strong electrostatic forces. Zeolite surfaces possess acidic silanol groups and a large number of cations which can interact electrostatically with guest molecules and these interactions may play significant role in controlling the fate of a photo-exited molecule.

Transition metal cations exchanged in zeolites tend to be isolated in the cavities and channels of zeolites [5–13]. Anpo et al. have used Cu ion exchanged ZSM-5 as an effective photocatalyst for decomposition of NO [6]. Also Pr [7], Ag [8] and Fe [9] exchanged zeolites have been reported to act as photocatalysts for N_2O decomposition. BEA zeolite was used as a support for several transition metal oxides because of its large-pore window [14,15].

Recently, Chatti et al. used Ti on Y zeolite for the photoreduction of methyl orange [16], and Mohamed et al. [17] used Ti/ZSM-5 catalyst for the photodegradation of EDTA. Othman et al. [18] synthesized Mn and La-modified ZSM-5 for the decolorization of indigo carmine dye.

In the present work, the metals: V, Cr, Mn, Cu or Zn have been exchanged in zeolites ZSM-5, MOR or Y to be used as photocatalysts for photodegradation of *n*-hexadecane (*n*-C_{16}) in water in presence of visible irradiation. Langmuir–Hinshelwood kinetics enabled direct calculation of the photocatalytic degradation rate constant, *k*, and the coefficient of adsorption, K_{ad}, on the prepared catalysts. The catalysts have been characterized using UV/vis, Fourier transform infrared (FTIR) and X-ray diffraction (XRD) spectroscopy.

* Corresponding author.
E-mail address: aboulgheit2000@hotmail.com (A.K. Aboul-Gheit).

1381-1169/$ – see front matter © 2008 Elsevier B.V. All rights reserved.
doi:10.1016/j.molcata.2008.03.016

Table 1
Transition metals exchanged in zeolite Y to ~5.2 wt%

Exchanged metal	Metal (wt%)	Metal exchange level (mol%)
V	5.17	96
Cr	5.23	97
Mn	5.17	64
Cu	5.22	56
Zn	5.19	54

2. Experimental

2.1. Preparation of photocatalysts

Three zeolites, namely Na–MOR, Na–ZSM-5 and Na–Y were exhaustively exchanged with molar NH_4NO_3 solution four times each for 8 h at ambient temperature with continuous stirring for complete replacement of Na^+ with NH_4^+. The zeolite was washed with deionized water till complete removal of NO_3^- ions. Each NH_4-zeolite was then exchanged with vanadium(III) chloride, chromium(III) chloride, manganese chloride, copper(II) chloride or zinc chloride to the extents listed in Table 1, such that the metal exchanged was ~5.2 wt% in all catalysts. The catalysts were thoroughly dried at 110 °C overnight then calcined at 400 °C for 4 h.

2.2. Characterization of photocatalysts

The exchanged metal contents were determined by inductively coupled plasma (ICP) spectroscopy using ARI Fisons 3410+ICP equipment. The UV/vis spectra for the metals-exchanged Y zeolite catalysts were measured using HP 8452A diode array spectrophotometer. The FTIR spectra for these catalysts were measured using Fourier transform infrared ATI Mattson Gensis FTIR™. The XRD patterns for the current catalysts were carried out using Bruker D8-ADVANCE equipment with an X-ray source of Cu K radiation at $\lambda = 1.5418$ Å. The X-ray tube was operated at 30 kV and 20 mA and the samples were scanned from $2\theta = 4^\circ$ to 90°.

2.3. Photocatalytic degradation procedure and apparatus

The photocatalytic reaction was carried out in a pyrex cylindrical batch reactor containing n-C_{16} at molar concentrations of 2.2, 3.0, 4.45 or 8.8 mol l^{-1} (initial concentration). A constant weight of 1.0 g l^{-1} of a catalyst powder was added in the solution. The irradiation source was a 200 W halogen lamp with wavelength ranging from 300 to 800 nm immersed inside the suspension and cooled by water circulation through a quartz jacket. A flow of 25 cm^3 min^{-1} of air was continually pumped and a magnetic stirrer was continuously working at the bottom of the reaction solution. A fixed irradiation period of 2 h was always used for each run. The concentration of n-C_{16} was estimated by gas chromatography.

3. Results and discussion

Since diffusion of a guest molecule in the intracrystalline cavities and channels of a zeolite occurs only when the kinetic diameter of the guest is smaller than the diameter of the cavity, we have chosen an alkane "n-hexadecane" in order to exclude significant diffusion restriction. Like other n-alkanes, n-hexadecane acquires a diameter of 4.6 Å which is smaller than that of the ZSM-5 zeolite channels which possess dimensions of 5.1 Å × 5.6 Å. Nevertheless, zeolites Y and MOR possess larger channel diameters, and hence diffusion in these channels does not encounter resistance. This choice of a guest molecule and the zeolites can be assumed to realize closer contact of the guest molecule with the exchanged cations in the intracrystalline cavities and channels of the zeolites. In previous work [19,20], the authors show that alkanes are significantly less reactive than aromatics and naphthenes (cycloparaffins); which may also substantiate our choice of n-C_{16} as a substrate in this work.

The photodegradation of n-C_{16} has been tested in presence of photocatalysts containing MOR, ZSM-5 and Y zeolites exchanged with V, Cr, Mn, Cu or Zn which possess the atomic weights 50.94, 52.00, 54.94, 63.54 and 65.37, respectively. Since the photoreactions occurring within a zeolite is imagined to be within an enclosed space [21], where the exited reaction molecules and their intermediates are mobilized during their life-times, the available space volume for a molecule in a zeolite cavity or channel depends on the size and nature of the exchanged cation, it is logically expected that this space volume decreases as cation size increases, e.g., from Cr up to Zn possessing atomic weights of 52.00 and 65.37, respectively.

3.1. Characterization of the catalysts

3.1.1. UV/vis spectral analysis

The diffuse reflectance UV/vis spectra obtained for the metal-exchanged zeolite catalysts under study are shown in Fig. 1. The Cr-zeolite Y spectrum exhibits two absorption bands at 250 and 360 nm which are attributed to tetrahedrally coordinated CrO species that exists as an isolated state. Anpo and co-workers [11] in investigating a Cr-exchanged HMS mesoporous silica molecular sieve has realized the presence of three UV/vis excitation bands at 250, 360 and 480 nm. The disappearance of the 480 nm band in our present study on the Cr-zeolite Y may be attributed to the microporous nature. The bands at 250 and 360 nm may confer that charge transfer on the tetrahedrally coordinated moieties of Cr oxide involve transfer from O^{2-} to Cr^{6+}.

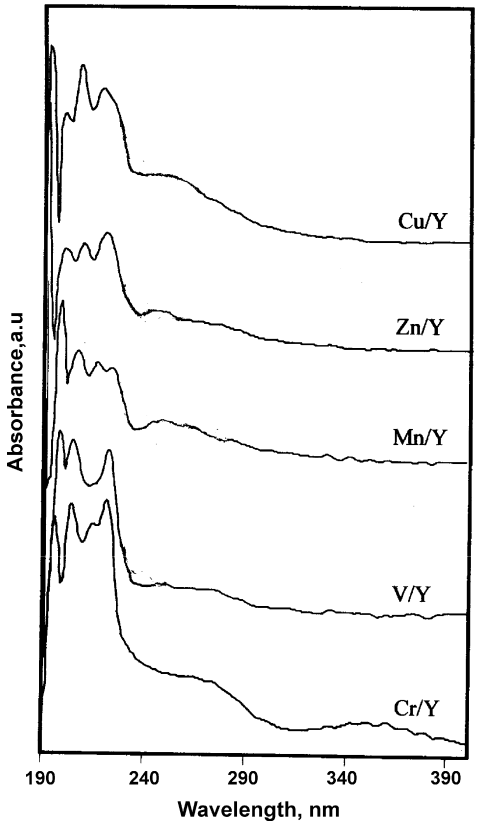

Fig. 1. UV/vis spectra for metal-exchanged zeolite Y photocatalysts.

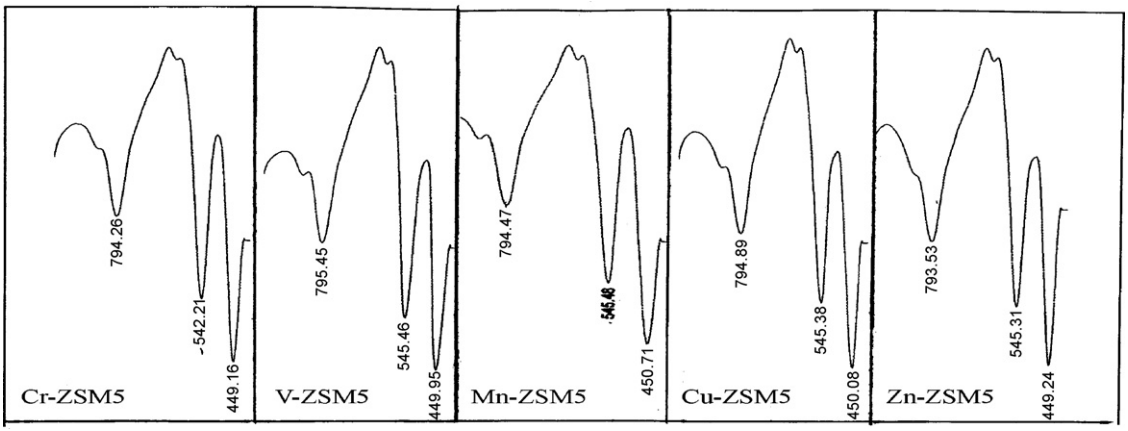

Fig. 2. FTIR spectra of metal-exchanged zeolite ZSM-5 photocatalysis.

The photoactive species of vanadium supported catalysts [22] is accepted to be considered as isolated vanadate with the specific structure of tetrahedral VO_4 with mono-oxo-species. In Fig. 1, not only the vanadium-exchanged zeolite Y depicts a UV/vis band at 250 nm, but also the Cu, Zn and Mn-exchanged zeolite Y catalysts which indicate isolated metal oxide species in the zeolite cavities and channels. These results also suggest that the immobilization of the metals in the zeolites improves the photooxidation and that these metals tend to be isolated. Several authors [5–13] show that the isolated metals can act as active sites for various photocatalytic reactions.

3.1.2. FTIR spectral analysis

The FTIR spectra of the current metal-exchanged zeolite catalysts during the region 400–550 cm^{-1} were determined and the skeletal vibrations of MFI zeolite structure [23] appear. The band at 550 cm^{-1} is assigned to the vibration of the double 5-rings in MFI lattice, and the ratio of intensities of the bands at 500 and 450 cm^{-1} is indicative of the zeolite crystallinity [24]. These values of the ratios have been assumed to amount to ~0.8 for pure samples. In this work, the ratio of the intensities of these bands amount to ~1/1 (Fig. 2), indicating high crystallinities of the current metal-exchanged H-ZSM-5 catalysts.

3.1.3. X-ray diffraction spectral analysis

The XRD powder diffraction patterns of the metals-exchanged zeolite catalysts. The zeolites under study have been exchanged with chlorides of the respective metals whereby in all of the obtained catalysts, the metal contents are always controlled to be 5.0 wt% (Table 1), since the catalytic activities of these catalysts are dependent on the metal loading. The penetration of the exchanging precursor solution into the zeolitic channel and cavities has been assisted by addition of citric acid [25]. The metal zeolite catalysts prepared have been calcined at 550 °C for 4 h in a current of air of 50 cm^3 min^{-1} in order to transform all exchanged metals to the corresponding oxides. All of the XRD patterns obtained for the current catalysts have been found indifferent from the unloaded mother Na-zeolites (Na–ZSM-5, Na–MOR or Na–Y). Although these metal contents are not very low, the XRD characteristic peaks for the metals did not appear which is attributed to high dispersion of these metals in the channels and cavities of the zeolites, i.e., the particle sizes of these transition metal oxides are significantly low.

3.2. Photocatalytic degradation of n-hexadecane in water

All of the current unloaded zeolites are not found to exhibit any photocatalytic activitiy for degrading of n-C_{16}, indicating the necessity of the presence of a transition metal in the zeolites. On the other hand, all metal loaded zeolites exhibited varying activities. As these catalysts are in the form of powdered heterogeneous catalysts, application of the Langmuir–Hinshelwood kinetics (Eq. (1)) is justified to be applicable.

$$\text{rate, } r = \frac{kK_{ad}C_0}{1 + K_{ad}C_0} \quad (1)$$

Plots of $1/r$ vs. $1/C_0$ for n-C_{16} photodegradation in water using the current catalysts containing the above-mentioned transition metals exchanged in the zeolites MOR, ZSM-5 or Y, are found to be elegantly linear (Fig. 3), indicating that Eq. (1) appropriately applies. C_0 is the initial concentration of n-C_{16}. The linearity of these plots can be considered as a proof of the absence of diffusion limitation. The intercept and slope of the linear plots represent the reciprocals of k and kK_{ad}. However, it is found that the k values obtained for n-C_{16} degradation using the catalysts containing Cr, Mn, Cu or Zn exhibit measurable systematic variations, whereas for the catalysts containing vanadium exchanged in the three current zeolites (Fig. 3a), the k values are insignificantly different (ranging between 8.0 and 8.6×10^{-3} min^{-1} g^{-1}), i.e., the effect of changing the zeolite type is insignificant. Machej et al. [26] assumed that all supported V catalysts contain the same vanadium oxide configuration after calcinations. Wang et al. [27] and Weckhuysen and Keller [28] proposed the formation of monolayer surface vanadium oxide species on the surface of different supports during hydrocarbons oxidation. These findings seem being compatible with our vanadium photocatalytic data.

The calculated k values have been plotted vs. the atomic weights of the metals exchanged in the current zeolites (Fig. 4). Evidently, n-C_{16} photodegradation is highest using the metal-exchanged MOR catalysts, but lowest using the metal-exchanged Y zeolite catalysts, i.e., the activities are in the order: M/MOR > M/ZSM-5 > M/Y, where M is the exchanged metal cation. Nevertheless, the photocatalytic effectiveness of the current metals is found to increase almost linearly as the atomic weight of the exchanged cation decreases, only when the host zeolite is MOR. On the contrary, when the host zeolite is either ZSM-5 or Y, the effectiveness of the metals behaves in an opposite direction, i.e., increases with increasing the metal atomic weight. In addition, Shimizu et al. [14] in their data for benzene photo-oxidation using metals-exchanged zeolite

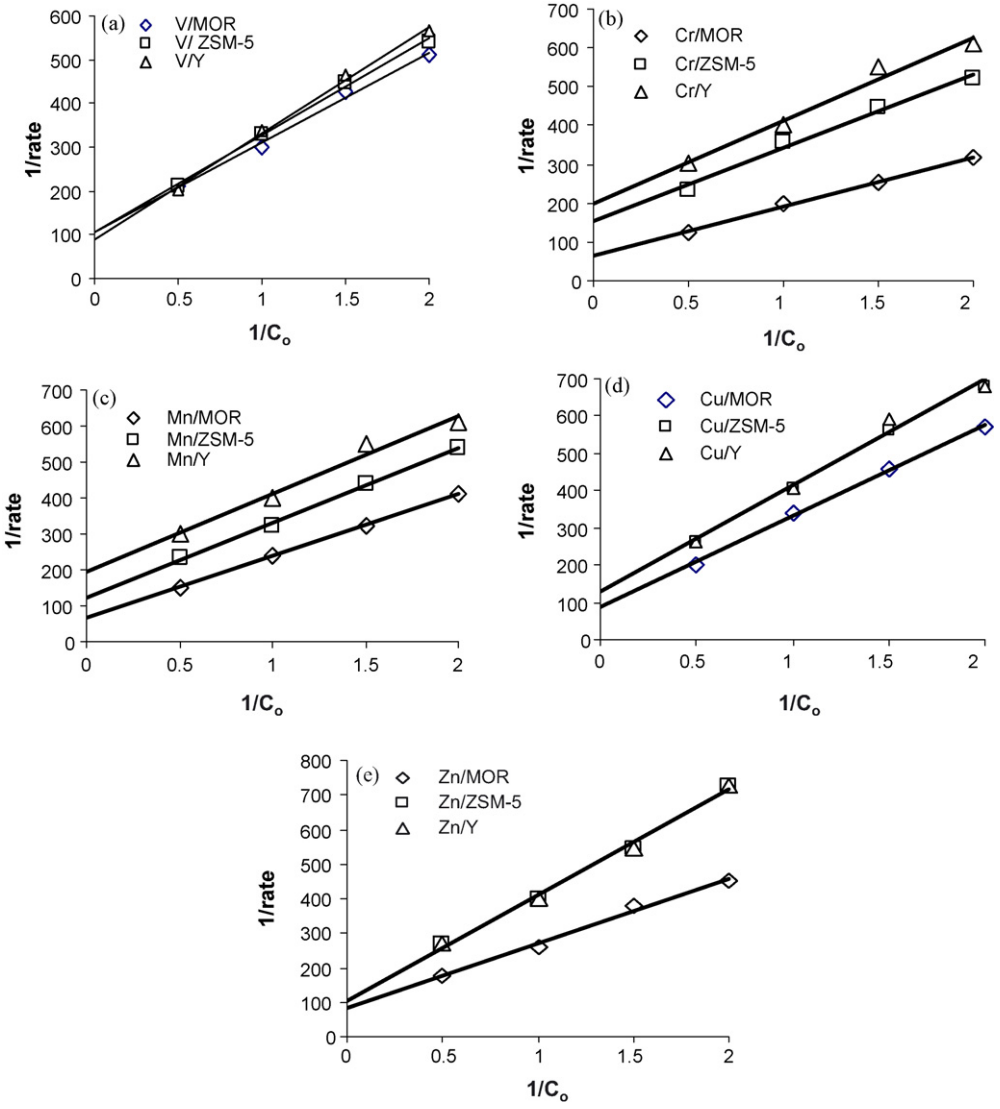

Fig. 3. Photocatalytic degradation of n-C_{16} using (a) vanadium, (b) chromium, (c) manganese, (d) copper and (e) zinc supported on MOR, ZSM-5 and Y zeolites catalysts.

BEA, have found that CO_2 evolved as a result of complete photo-oxidation of benzene to be in the order: Mn/BEA > Cu/BEA > Zn/BEA, which is compatible with our data using the metals/ZSM-5 and metals/Y catalysts, but not with metals/MOR catalysts. Zeolite BEA acquires open 12-member rings intersecting channels with 6.5 Å × 5.6 Å and 7.5 Å × 5.7 Å dimensions. This channel-structure of BEA resembles those of zeolites Y and ZSM-5 but not MOR which should contribute to difference in the trend of k values with the metals atomic weights (Fig. 4). Nevertheless, MOR is orthorhombic with 8- and 12-member rings (6.5 Å × 7.0 Å and 2.6 Å × 5.7 Å). MOR zeolite contains a two-dimensional channel system, but for practical application it is considered to be a unidimensional large-pore molecular sieve with side pockets, because of the constraint on the 8-member rings openings for diffusion. The main cage is defined by two 4 rings and two hexagonal sheets connected by them. This case has two exits, through two 8-member rings [29].

Joyner and Pendry [30] in their study for estimating minimum poison or promoter required for individual metals, have calculated the area occupied by the active surface of each individual metal atom, A in Å^2, applying the following equation:

$$\mathrm{SA} = \frac{LNAD}{W_\mathrm{m} 1 \times 10^{20}} \tag{2}$$

where SA is the surface area of the metal per gram of catalyst, L is the metal loading (wt%), N is the Avogadro's number, D is the percentage dispersion of the metal and W_m is the atomic weight of the metal. Fig. 5 is a plot of the atomic weights of the current metals vs. the respective active atomic surface areas calculated by Joyner and Pendry [30]. This relationship is elegantly linear and inversely proportional, i.e., as the weight of a metal atom increases, its active surface area decreases. Considering the correctness of Joyner and Pendry calculations, we have plotted our photocatalytic degradation k values (obtained applying the Langmuir–Hinshelwood Eq. (1)) vs. the area occupied by the active surface of metal atoms. Fig. 6 shows again that the order of the k values with respect to the zeolites is the same as in Fig. 4; i.e., M/MOR > M/ZSM-5 > M/Y (where M is a metal cation), but the increase or decrease of k as a function of active atomic surface area is reversed.

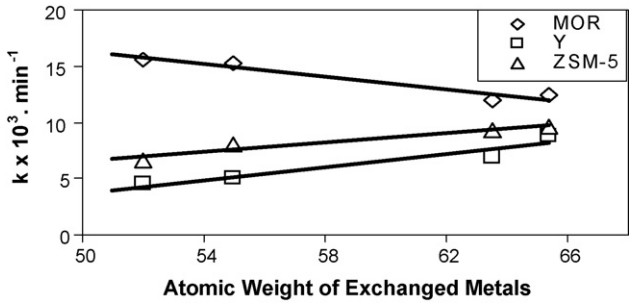

Fig. 4. Effect of atomic weight of exchanged metals in zeolites on n-C_{16} photodegradation rate constant, k.

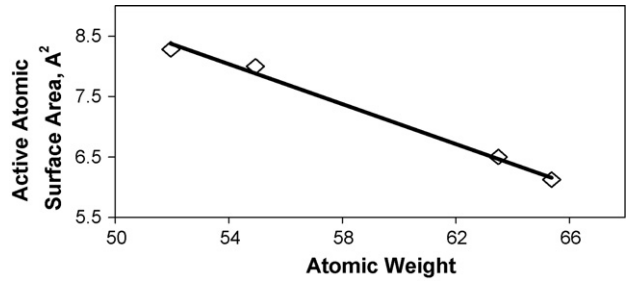

Fig. 5. Change of active atom surface area with the metal atomic weight.

Since the active surface area of a metal is primarily dependent on the amount of metal exchanged in a zeolite, it is necessary to have all metals-exchanged zeolite acquiring the same weight of the different metals. Table 2 shows that V and Cr have been exchanged almost completely in the available cationic sites of zeolite Y, whereas Mn, Cu and Zn have been exchanged to mol percent levels of 64, 56 and 54, respectively, such as to keep the same weight percent level of the metals, under study at ~5.2%.

It deserves mentioning that in a previous communication [31] we have investigated n-C_{16} photodegradation using the group VIII metals (Fe, Co and Ni) exchanged in the current zeolites (MOR, ZSM-5 and Y). As a trial to compile the k values obtained for Cr, Mn, Fe, Co, Ni, Cu and Zn (as members of the same period) in the current zeolites, we did not find that Fe, Co or Ni conform to those obtained in the present investigation using Cr–Zn metals in Figs. 4 and 6. Even if the active atomic surface area values, calculated by Joyner and Pendry [30] for Fe, Co and Ni are located in the plot in Fig. 6, they will show distinct deviation, indicating that group VIII metals (1st period) may have a special situation that may require further investigation.

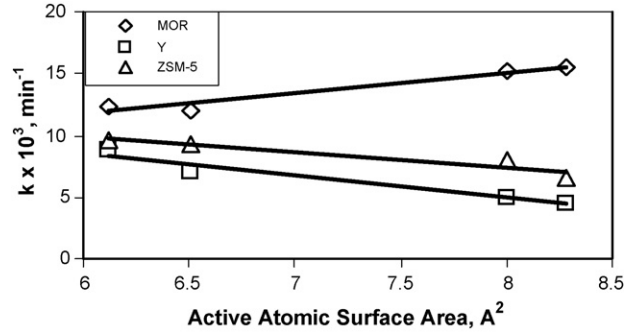

Fig. 6. Effect of the active atomic surface area on the k values of n-C_{16} photodegradation.

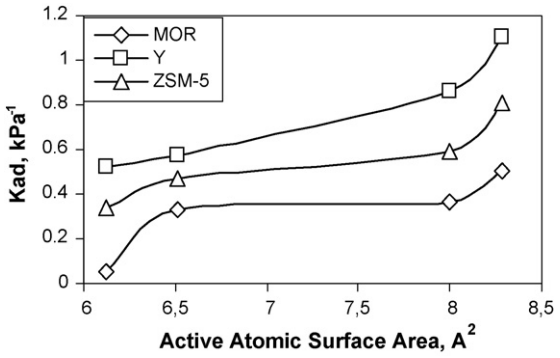

Fig. 7. Effect of the active atomic surface area on the adsorption coefficient, K_{ad} of n-C_{16} photodegradation.

Actually, it seems significantly relevant to examine the relationship between the adsorption coefficient, K_{ad}, calculated applying the Langmuir–Hinshelwood Eq. (1) and the active metal atomic surface areas [30]. Fig. 7 shows that the adsorption coefficient values, generally, increase as the active surface area of the exchanged metal increases. The order of this coefficient with respect to the host zeolite is as follows: M/Y > M/ZSM-5 > M/MOR, which is compatible with the properties of the zeolites. Zeolite Y acquires the highest void volume (0.48 $cm^3\,g^{-1}$ compared to 0.29 and 0.28 $cm^3\,g^{-1}$ for the ZSM-5 and MOR, respectively). Also, the surface area of the zeolite Y is highest (622 $m^2\,g^{-1}$) relative to 560 and 355 $m^2\,g^{-1}$ for ZSM-5 and MOR, respectively. Zeolite Y includes large-pore three-dimensional 12-member ring pores with 7.4 Å × 6.5 Å (cubic) dimensions; whereas zeolite ZSM-5 possesses medium-pore three-dimensional intersecting 10-member ring pores with 5.3 Å × 5.6 Å and 5.1 Å × 5.5 Å dimensions. Moreover, the larger channel dimensions in Y zeolite than in ZSM-5 zeolite substantiate larger K_{ad} using Y than ZSM-5. The evident diffusion constraint in MOR structure may be the main reason for acquiring the lowest values of K_{ad} among the current photo-catalysts. Even though, at the same time, the unidimensional large-pore structure may contribute to acquiring the highest k values using the M/MOR catalysts compared to the other current catalysts. Moreover, the M/MOR catalysts only exhibit a different trend, i.e., the k values decrease with increasing the atomic weights of exchanged metals (Fig. 4).

4. Conclusion

Characterization of the current catalysts indicated that they have their metals as isolated species (UV/vis diffuse reflectance spectroscopy) and their crystalinity is quite high (FTIR and XRD). Calculation of the rate constant and adsorption coefficient of n-C_{16} during its photocatalytic degradation applying the Langmuir–Hinshelwood kinetics enabled us to correlate the metals atomic weights and the active metals surface areas. The behaviour of increasing or decreasing the catalytic activities of the current catalysts according to the position of the metals in the periodic system (atomic weights) is found to be systematically linear. The correlation of activities (k values) or adsorption coefficients (K_{ad}) is found to be of the same direction for the metals loaded on ZSM-5 and Y zeolites but in apposite direction for the metals loaded on MOR catalysts which is most probably due to difference in the zeolitic pore structure (tridirectional vs. unidirectional). The metal and the zeolite both contribute to the photocatalytic activity of the catalyst. The unloaded zeolites are photocatalytically inactive.

References

[1] J.C. Jansen, M. Stocker, H.G. Karge, J. Weitkamp (Eds.), Advanced Zeolite Science and Applications, Elsevier, Amsterdam, 1994.
[2] N. Herron, D.R. Corbin (Eds.), Inclusion Chemistry with Zeolites: Nanoscopic Materials by Design, Kluwer Academic Publishers, Dordrechet, 1995.
[3] C.P. Grey, F.I. Poshni, A.F. Gaultieri, P. Norby, J.C. Hanson, D.R. Corbin, J. Am. Chem. Soc. 119 (1997) 1981.
[4] A.U. Munk, J.F. Scott, Nature 177 (1956) 587.
[5] H. Yoshida, C. Murata, T. Hattori, J. Catal. 194 (2000) 364.
[6] M. Anpo, M. Matsuoka, Y. Shioya, H. Yamashita, E. Giamello, C. Morterra, M. Che, H.H. Patterson, S. Webber, S. Ouellette, M.A. Fox, J. Phys. Chem. 98 (1994) 5744.
[7] K. Ebitani, Y. Hirano, A. Morikawa, J. Catal. 157 (1995) 262.
[8] M. Matsuoka, W.-S. Ju, M. Anpo, Chem. Lett. (2000) 626.
[9] S. Higashimoto, K. Nishimoto, T. Ono, M. Anpo, Chem. Lett. (2000) 1160.
[10] K. Teramura, T. Tanaka, T. Yamamoto, T. Funabiki, J. Mol. Catal. A 165 (2001) 299.
[11] H. Yamashita, K. Yoshizawa, M. Ariyuki, S. Higashimoto, M. Che, M. Anpo, Chem. Commun. (2001) 435.
[12] A. Maldotti, A. Molinari, R. Amadelli, Chem. Rev. 102 (2002) 3811.
[13] K. Fujishima, A. Fukuoka, A. Yamagishi, S. Inagaki, Y. Fukushima, M. Ichikawa, J. Mol. Catal. A 165 (2001) 299.
[14] K. Shimizu, H. Akahane, T. Kodama, Y. Kitayama, Appl. Catal. A: Gen. 269 (2004) 75.
[15] S. Anandan, A. Vinu, N. Venkatachalam, B. Arabindoo, V. Murugesan, J. Mol. Catal. A: Chem. 256 (2006) 312.
[16] R. Chatti, S.S. Rayalu, N. Dubey, N. Labhsetwar, S. Devotta, Sol. Energy Mater. Sol. Cells 91 (2007) 180.
[17] R.M. Mohamed, A.A. Ismail, I. Othman, I.A. Ibrahim, J. Mol. Catal. A: Chem. 238 (2005) 151.
[18] I. Othman, R.M. Mohamed, I.A. Ibrahim, M.M. Mohamed, J. Appl. Catal. A 299 (2006) 95.
[19] A.K. Aboul-Gheit, A.M. Badawi, S.M. Abdel-Hamid, S.M. Ahmed, 14th International Petroleum Conference on Downstream, vol. 2, Cairo, 1998, p. 268.
[20] A.K. Aboul-Gheit, A.M. Badawi, S.M. Abdel-Hamid, E.A. El-Sawi, S.M. Ahmed, 5th International Conference on Solar Energy and Applied Photochemistry, Photoenergy Center, Ain Shams University, Cairo, 1998.
[21] V. Ramamurthy, J. Photochem. Photobiol. C: Photochem. Rev. 1 (2000) 145.
[22] K. Teramura, T. Tanaka, T. Yamamoto, T. Funabiki, J. Mol. Catal. 165 (2001) 299.
[23] J.C. Jansen, F.J. van der Gaag, H. van Bekkum, Zeolites 4 (1984) 396.
[24] G. Coudurier, C. Naccache, J.C. Vedrine, J. Chem. Soc. Chem. Commun. (1982) 1413.
[25] A.K. Aboul-Gheit, J. Chem. Technol. Biotechnol. 29 (1979) 480.
[26] T. Machej, J. Haber, A.M. Turek, I.E. Wachs, Appl. Catal. 70 (1991) 115.
[27] C.B. Wang, Y. Cai, I.E. Wachs, Langmuir 15 (1999) 1223.
[28] B.M. Weckhuysen, D.E. Keller, Catal. Today 78 (2003) 25.
[29] R. Szostak, Handbook of Molecular Sieves, Van Nostrand Reinhold Publ., 1992.
[30] R.W. Joyner, J.B. Pendry, Catal. Lett. 1 (1988) 1.
[31] A.K. Aboul-Gheit, S.M. Ahmed, S.A. Hanafy, Trans. Egypt Soc. Chem. Eng. 29 (2003) 98.